

# Large-Signal Network Analysis for Over-the-Air Test of Up-Converting and Down-Converting Phased Arrays

Alec J. Weiss<sup>#1</sup>, Dylan F. Williams<sup>#2</sup>, Jeanne Quimby<sup>#3</sup>, Rod Leonhardt<sup>#4</sup>, Thomas Choi<sup>\$5</sup>, Zihang Cheng<sup>\$6</sup>, Kate A. Remley<sup>#7</sup>, Andreas Molisch<sup>\$8</sup>, Benjamin Jamroz<sup>#9</sup>, Jake Rezac<sup>#10</sup>, Peter Vouras<sup>#11</sup>, Charlie Zhang<sup>\*12</sup>

<sup>#</sup>National Institute of Standards and Technology, Boulder, CO USA

<sup>^</sup>Colorado School of Mines, Golden, CO USA

<sup>\$</sup>University of Southern California, Los Angeles, CA USA

<sup>\*</sup>Samsung Electronics, Richardson, TX USA

<sup>1</sup>alec.weiss@nist.gov, <sup>2</sup>dylan.williams@nist.gov, <sup>3</sup>jeanne.quimby@nist.gov, <sup>4</sup>leonhardt@nist.gov, <sup>5</sup>choit@usc.edu, <sup>6</sup>zihangch@usc.edu, <sup>7</sup>kate.remley@nist.gov, <sup>8</sup>molisch@usc.edu, <sup>9</sup>ben.jamroz@nist.gov, <sup>10</sup>jacob.rezac@nist.gov, <sup>11</sup>peter.vouras@nist.gov, <sup>12</sup>jianzhong.z@samsung.com

**Abstract**— We explore large-signal network analysis for the over-the-air test of up-converting and down-converting phased arrays. The approach first uses a vector network analyzer to characterize a three-dimensional test environment at RF. The vector network analyzer is then power- and phase-calibrated for the characterization of up-converting and down-converting phased arrays with an IF input or output. We illustrate the approach with measurements of a down-converting phased array.

**Keywords**— down-converter, large-signal network analysis, over-the-air test, phased array, phase calibration, spatial channel, up-converter, vector network analyzer, wireless system.

## I. INTRODUCTION

We present a practical approach for calibrating an over-the-air (OTA) test system with a vector network analyzer and then applying it to the characterization of up-converting and down-converting phased arrays. We accomplish this by use of a vector network analyzer (VNA) configured to operate as a large-signal network analyzer (LSNA) capable of performing calibrated amplitude and phase measurements across different frequency bands. This approach allows the VNA to first calibrate a static free-field channel in the OTA test system at RF frequencies, and then to characterize the response of the phased array at its connectorized IF port when it is inserted in that same channel. The approach is equally applicable to the characterization of up-converting IF-RF and down-converting RF-IF phased arrays without accessible RF ports between the phased-array elements and the converters.

We demonstrate the approach on a National Institute of Standards and Technology (NIST) OTA Test System, known as the Synthetic Aperture Measurement with Uncertainty and Angle of Incidence (SAMURAI) system, to characterize an experimental 28 GHz Samsung<sup>1</sup> up-converting and down-converting phased array [1]. This system consists of an LSNA, cables, antennas and a scanning positioner for the receive antenna. The SAMURAI system is focused on using synthetic aperture measurements at millimeter-wave frequencies to

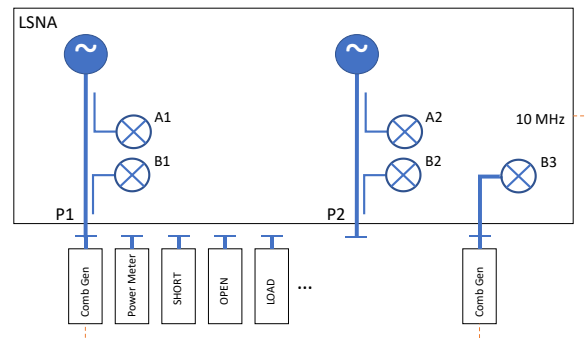


Figure 1. Simplified sketch of an LSNA and its calibration.

determine angle of arrival and other aspects of the channel for OTA test.

## II. LSNA CALIBRATION

Large-signal network analyzers are vector network analyzers configured both to determine conventional scattering parameters from the ratios of the forward and backward waves at their measurement ports and also to measure the amplitudes and “cross-frequency” phases of those forward and backward waves at their measurement ports. This greatly increases the utility of the VNA [2]. LSNA’s now find application not only in the characterization of nonlinear transistors, amplifiers and other devices [3, 4], but in modulated-signal characterization [5], mixer characterization [6-9], and the characterization of distortion in devices excited by modulated signals [10-12].

Figure 1 shows a simplified sketch of a typical two-port LSNA and illustrates its calibration sequence. The LSNA is first calibrated with conventional VNA scattering-parameter calibration artifacts (short, open, load, thru, etc.) at its two ports. Then, the power meter is used to measure the power on port 1 with the LSNA’s port 1 source turned on. The readings on the A1 and B1 receivers are compared to the power-meter reading

<sup>1</sup> The National Institute of Standards and Technology does not endorse commercial products. We use brand names only to better describe the experiments. Other products may work as well or better.

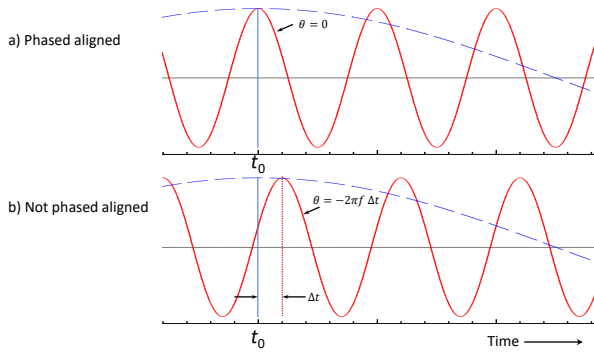


Figure 2. LSNA phase relationships between the lowest IF frequency (blue dashed line) and a higher frequency (red solid line) signals.

to establish the relationships between the forward and backward wave amplitudes at the ports of the LSNA and perform the LSNA's power calibration [2].

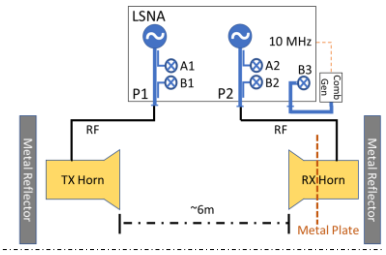
Finally, the LSNA's cross-frequency phase calibration is performed to establish the phase relationships across different frequency bands measured by the LSNA. In essence, the LSNA is calibrated to measure the phases of the forward and backward waves at different frequencies with respect to a single fixed time zero. In our case, this aspect of the calibration required the use of two comb generators, each triggered with the 10 MHz reference of the LSNA. These comb generators create a comb of phase-stable tones at multiples of 10 MHz.

The first of these comb generators is connected to the LSNA's receiver B3 and is left on during the entire calibration and measurement sequence. This comb generator provides a stable but unknown set of tones to which the LSNA references all its measurements. That is, the LSNA is configured to perform raw measurements on each of its receivers simultaneously, and then set a uniform time reference by dividing these raw complex receiver measurements acquired on A1, B1, A2, and B2 by  $b_3/|b_3|$ , where  $b_3$  is the measurement performed on B3 at the same frequency. This operation is performed before any other processing of the data is performed.

To complete the cross-frequency phase calibration, the source connected to port 1 is switched off, and a calibrated comb generator that creates tones with already characterized electrical phases is connected to port 1 of the LSNA, as illustrated in Fig. 1. The measurements on A1 and B1, after normalization by  $b_3/|b_3|$ , are compared to the known response of the comb generator to perform the phase calibration. The phase relationships between the tones generated by this comb generator were characterized by a sampling oscilloscope that was calibrated with an electrooptic sampling system [13, 14].

In the final step of the phase calibration, the time zero  $t_0$  for the LSNA measurements is set to the time at which the phase of the incoming wave on port 1 from the comb generator at the lowest frequency in the calibration (the lowest-frequency IF component in this case) is set equal to zero, as illustrated by the dashed blue line in Fig. 2. The solid red line in Fig. 2 illustrates how the phases of a second forward or backward wave at a different frequency are then related to the phase of the first wave after calibration. If the peak voltage of the second wave aligns perfectly in time with the peak voltage of the first wave

(a) OTA Test System Measurement Setup



(b) Samsung Array Measurement Setup

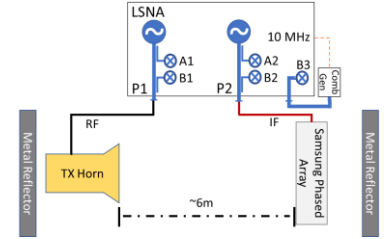


Figure 3. The measurement configuration. Optional metal plate added for measurements in Figure 5.

at the lowest frequency in the calibration, as illustrated in Fig. 2(a), the phase  $\theta$  of the second wave is zero. However, if the peak of the second wave was offset by  $\Delta t$ , as shown in Fig. 2(b), the phase of the second wave would be  $\theta = -2\pi f \Delta t$ .

For our application, the phase calibration was performed over all the RF and IF frequencies that were used in the experiment, establishing their phases with respect to a single point in time and forming the basis for determining the RF-IF frequency response of the phased array.

### III. NIST OTA TEST SYSTEM

Figure 3 shows the NIST OTA Test System. The LSNA performs all the electrical measurements in the system. After calibration, the LSNA is first used as a conventional VNA, where the output frequency is assumed to equal the input frequency, to characterize the RF environment in the NIST OTA Test System. Here, we don't require the cross-frequency phases. However, to simplify the overall calibration approach, the RF scattering parameters are determined from the magnitudes and phases of the forward and backward waves at the ports of the LSNA, as shown in Fig. 3(a). The calibrated horn on the right can be scanned to perform synthetic-aperture and other measurements that characterize angle and time of arrival, and other characteristics of the three-dimensional RF environment (sometimes called the "spatial channel") between the horns.

After the RF environment has been characterized, the horn and positioning system on the right are replaced by the phased array, as illustrated in Fig. 3(b), and the amplitude and phase calibrations of the LSNA come into play. When characterizing a down-converting phased array, the LSNA measures the IF response of the array in the configuration shown in Fig. 3(b) relative to the RF free-field excitation characterized by the LSNA in the configuration shown in Fig. 3(a). Since the LSNA is capable of measuring both the amplitudes and phases of the array's IF output signals compared to the amplitudes and phases of the array's RF input signals, it can construct the RF-to-IF power-delay-profiles (PDPs) measured by the down-converting

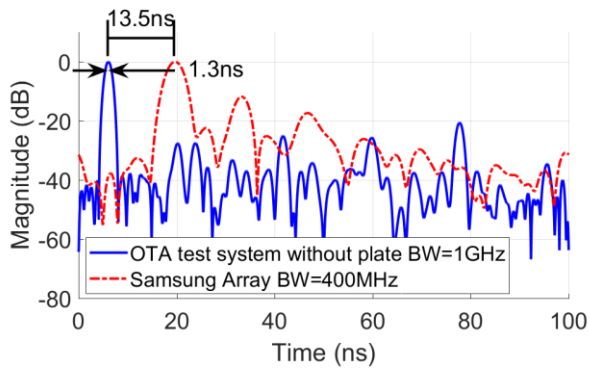


Figure 4. Comparison of the measured OTA boresight RF-RF (solid) and Samsung RF-IF (dashed) PDPs.

phased array and the frequency and impulse responses of the down-converting phased array as described in [8].

Characterizing the frequency and impulse responses of an up-converting phased array is performed in the same way, except that the IF-RF up-converting performance of the phased array is tested.

#### IV. SAMSUNG PHASED-ARRAY MEASUREMENT DEMONSTRATION

We calibrated the LSNA and performed a series of tests to explore its use within the NIST OTA Test System. We used a 28 GHz experimental up-converting and down-converting Samsung phased array with a 400 MHz bandwidth for the demonstration [1]. We tested the array in its down-converting mode of operation in the reflective environment between the two metal reflectors sketched in Fig. 3.

For these experiments, we first used the LSNA to characterize the three-dimensional RF channel with a pair of Sage-Millimeter<sup>2</sup> 26.5-40 GHz, 23 dBi, WR 28 horns over a 1 GHz frequency range spanning 27.65 GHz to 28.65 GHz. This horn was selected because it has a beamwidth similar to that of the Samsung array. Then we replaced the RX horn, which has a small form factor, with the much larger Samsung array and measured its RF-to-IF characteristics over the 400 MHz frequency range spanning 27.65 GHz to 28.05 GHz in the same highly reflective environment. For these measurements, the Samsung array was physically positioned to point directly at the horn and its beam was electronically steered to boresight.

Figure 4 compares the RF-RF PDP measured by the NIST OTA Test System with the full 1 GHz bandwidth, which includes the response of the WR-28 RX horn and the RF-IF PDP measured by the Samsung array over its smaller 400 MHz bandwidth. For this comparison, both peaks of the PDP were normalized to 0 dB (amplitude comparisons were not meaningful due to unknown gain and loss in the IF amplifiers and other electronics integrated into the Samsung array).

While the levels of the multipath components measured by the NIST OTA Test System in this reflective environment were much higher than we see in quieter environments, the 1 GHz bandwidth, 1.3-ns wide, 3-dB response of the test system to the first line-of-sight component is significantly sharper than that of the 400 MHz bandwidth, 3.2 ns wide, 3 dB response of the Samsung array. This is expected due to the different bandwidths

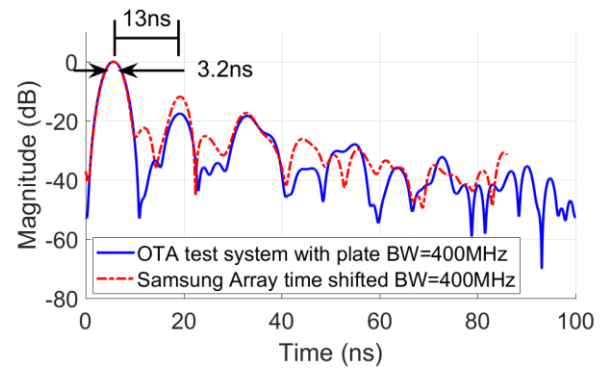


Figure 5. Comparison of the measured boresight OTA RF-RF and Samsung RF-IF PDPs after reducing the OTA-test-system bandwidth to 400 MHz, adding an optional metal plate behind the OTA horn (this boosts the first multipath component 13 ns after the first line-of-sight pulse), and shifting the arrival time of the first line-of-sight impulse measured by the Samsung array to 6 ns.

of the systems. The 6-ns arrival time of the first line-of-sight component measured by the NIST OTA Test System was also very close to what we expected, based on the roughly two-meter distance between the two horns. However, the arrival time of the first line-of-sight component measured by the Samsung array was delayed by an additional 13.5 ns due to the internal electronics in the array. This example illustrates the ability of the LSNA to track the phases (and timing) during both the RF-RF system characterization and the ensuing RF-IF array measurement.

In Fig. 5, we were able to improve the comparison and explain most of the discrepancy between the two measurements. This was done by reducing the bandwidth of the RF-RF NIST OTA Test System measurements to 400 MHz and adding a metal plate of the same size as the Samsung array's metal housing behind the horn, which increased the amplitude of the first multipath component. We also shifted the arrival time of the first line-of-sight component measured by the Samsung array to better compare measurements.

#### V. IMPACT OF LSNA UNCERTAINTY

While the overall uncertainty of the NIST OTA Test System is still being evaluated, we were able to estimate the impact of measurement errors due to the scattering-parameter and phase calibration, the LSNA's repeatability and drift, as determined from 10 repeat measurements, and cable bending, as determined from repeated measurements of the cables during

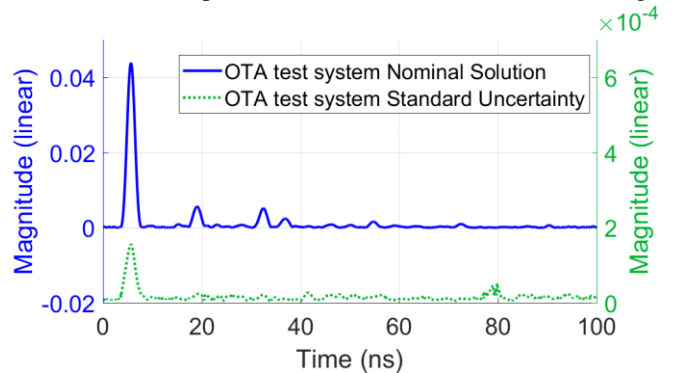


Figure 6. OTA test system PDP and its uncertainties. simulated measurements.

Figure 6 compares the uncertainty attributable to the LSNA measurements due to these factors. We used the NIST Microwave Uncertainty Framework [15] to capture the correlations in these frequency-domain uncertainties and propagate them through the Fourier transform to the time domain for comparison [16, 17]. The figure illustrates how the correlated uncertainty analysis performed by the Microwave Uncertainty Framework is able to temporally line up the uncertainty in the direct line-of-sight component with the arrival of the component itself. This is not possible in conventional frequency-point-by-frequency-point uncertainty analyses [18, 19].

The figure also shows that the error in the measurements attributable to the LSNA is quite low. Thus, we expect error in the NIST OTA Test System to be dominated by other sources, including characterization of the antenna responses, positioning errors, and interactions of the positioning equipment, cables and horns. These are the subject of future work.

## VI. CONCLUSION

We demonstrated the use of a VNA configured to operate as an LSNA for calibrated measurements as an OTA test system. We showed that the LSNA allows the system to be used both to perform RF-RF characterization tasks and RF-IF measurements that characterize the performance of up-converting and down-converting arrays in the test environment. These tests allow for the characterization of phased arrays without a connectorized RF port, including their hardware latency compared to that of the standard horn.

While we only showed measurements of the array in its down-converting mode of operation in a highly reflective environment, testing in a less-reflective environment would have provided a simpler and less-demanding RF environment for the array and de-emphasized the impact of the large array form factor on its frequency response.

In addition, the LSNA's RF-IF characterization can be used with the full synthetic-aperture capability of the NIST OTA Test System. Using fully characterized horn antennas together with the synthetic-aperture techniques of the NIST OTA Test System will allow us to precisely determine times and angles of arrival in the three-dimensional, spatial-channel test environment and develop a better understanding of the actual performance of up-converting and down-converting arrays.

## ACKNOWLEDGMENT

We thank Prof. Atef Elserbeni, Dobelman Distinguished Professor of Electrical Engineering at the Colorado School of Mines, for support of Alec Weiss and many helpful discussions.

## REFERENCES

- [1] C. U. Bas *et al.*, "A Real-Time Millimeter-Wave Phased Array MIMO Channel Sounder," in *2017 IEEE 86th Vehicular Technology Conference (VTC-Fall)*, 2017, pp. 1-6.
- [2] J. Verspecht, "Large-Signal Network Analysis," *IEEE Microwave Magazine*, vol. 6, no. 4, pp. 82-92, 2005.
- [3] J. Verspecht, "Calibration of a Measurement System for High Frequency Nonlinear Devices," *Ph.D.Thesis, Free University of Brussels*, 1995.
- [4] F. D. Groote, J. Teyssier, T. Gasseling, O. Jardel, and J. Verspecht, "Introduction to measurements for power transistor characterization," *IEEE Microwave Magazine*, vol. 9, no. 3, pp. 70-85, 2008.
- [5] N. B. Carvalho, K. A. Remley, D. Schreurs, and K. G. Card, "Multisine signals for wireless system test and design [Application Notes]," *IEEE Microwave Magazine*, vol. 9, no. 3, pp. 122-138, 2008.
- [6] J. Dunsmore, "Novel method for vector mixer characterization and mixer test system vector error correction," *IEEE MTT-S Int.Microwave Symp.Dig.*, vol. 3, pp. 1833-1836, 2002.
- [7] J. Dunsmore, S. Hubert, and D. F. Williams, "Vector mixer characterization for high-side LO cases," *IEEE MTT-S Int.Microwave Symp.Dig.*, vol. 3, pp. 1743-1746, 2004.
- [8] D. F. Williams, F. Ndagijimana, K. A. Remley, J. Dunsmore, and S. Hubert, "Scattering-parameter models and representations for microwave mixers," *IEEE Trans.Microw.Theory Techn.*, vol. 53, no. 1, pp. 314-321, 2005.
- [9] J. Dunsmore, "System for characterizing mixer or converter response," USA Patent US8744370B2, 2011.
- [10] J. Verspecht, F. Verbeyst, and M. Vanden Bossche, "Network Analysis Beyond S-parameters: Characterizing and Modeling Component Behaviour under Modulated Large-Signal Operating Conditions," *ARFTG Conference Digest*, vol. 56, pp. 1-4, 2009.
- [11] J. Verspecht, D. F. Williams, D. Schreurs, K. A. Remley, and M. D. McKinley, "Linearization of large-signal scattering functions," *IEEE Transactions on Microwave Theory and Techniques*, vol. 53, no. 4, pp. 1369-1376, 2005.
- [12] K. A. Remley, D. F. Williams, D. M. M. Schreurs, and J. Wood, "Simplifying and interpreting two-tone measurements," *IEEE Transactions on Microwave Theory and Techniques*, vol. 52, no. 11, pp. 2576-2584, 2004.
- [13] T. S. Clement, P. D. Hale, D. F. Williams, C. M. Wang, A. Dienstfrey, and D. A. Keenan, "Calibration of Sampling Oscilloscopes with High-Speed Photodiodes," *IEEE Trans.Microw.Theory Techn.*, vol. 54, no. 8, pp. 3173-3181, 2006.
- [14] H. C. Reader, D. F. Williams, P. D. Hale, and T. S. Clement, "Comb-Generator Characterization," *IEEE Transactions on Microwave Theory and Techniques*, vol. 56, no. 2, pp. 515-521, 2008.
- [15] D. F. Williams and A. Lewandowski, "NIST Microwave Uncertainty Framework," ed: National Institute of Standards and Technology, <http://www.nist.gov/ctl/rf-technology/related-software.cfm>, 2011.
- [16] K. A. Remley, D. F. Williams, P. D. Hale, C. M. Wang, J. Jargon, and Y. Park, "Millimeter-Wave Modulated-Signal and Error-Vector-Magnitude Measurement With Uncertainty," *IEEE Transactions on Microwave Theory and Techniques*, vol. 63, no. 5, pp. 1710-1720, 2015.
- [17] G. Avolio, A. Raffo, J. Jargon, P. D. Hale, D. M. M. Schreurs, and D. F. Williams, "Evaluation of Uncertainty in Temporal Waveforms of Microwave Transistors," *IEEE Trans.Microw.Theory Techn.*, vol. 63, no. 7, pp. 2353-2363, 2015.
- [18] D. F. Williams, P. D. Hale, T. S. Clement, and J. M. Morgan, "Calibrated 200 GHz Waveform Measurement," *IEEE Trans.Microw.Theory Techn.*, vol. 53, no. 4, pp. 1384-1389, 2005.
- [19] B. F. W. Jamroz, D.F.;Remley,K.A.;Horansky,R.D., "Importance of Preserving Correlations in Error-Vector-Magnitude Uncertainty," presented at the ARFTG Microwave Measurement Conference, Philadelphia, PA, 6/15/2018.